Article

Electrodynamics of Power Losses in the Devices of Inter-Substation Zones of AC Electric Traction Systems

Anatolii Nikitenko [1,*], Mykola Kostin [2], Tetiana Mishchenko [3] and Oksana Hoholyuk [4]

1 Division of Traction and Electrical Power Economics, Electrical Power Engineering Institute, Warsaw University of Technology, Koszykowa St. 75, 00-662 Warsaw, Poland
2 Department of Electrical Engineering and Electromechanics, Ukrainian State University of Science and Technologies, Lazaryana St. 2, 49-010 Dnipro, Ukraine; nkostin@ukr.net
3 Department of Intelligent Power Supply Systems, Ukrainian State University of Science and Technologies, Lazaryana St. 2, 49-010 Dnipro, Ukraine; mishchenko_tn@ukr.net
4 Department of Theoretical Electrical Engineering, Lviv Polytechnic National University, Bandery St. 12, 79-013 Lviv, Ukraine; oksana.p.hoholyuk@lpnu.ua
* Correspondence: anatolii.nikitenko@pw.edu.pl; Tel.: +48-2223-476-16

Abstract: This article presents a new method for the estimation of active power losses based on a "field" approach, i.e., on the theory of the electromagnetic field and the theory of propagation of electromagnetic waves in a dielectric medium. Electromagnetic waves are assumed to transmit energy from the traction substation to electric rolling stock through the airspace of the inter-substation zone (i.e., not through the wires of the traction network) and meet electrically conductive surfaces on their way. The waves are partially reflected from the surfaces and partially penetrate them, thus creating thermal losses, the determination of which is the main task of this article. The analytical expressions for specific losses of active power are obtained by solving the system of Maxwell's equations. Calculations of specific power losses in the catenary, rails, roofs, and bottoms of carriages and electric locomotives are performed. Power losses in carriages and electric locomotives are found to be at least 7%. A comparative assessment of the magnitude of total power losses of different types obtained by the "field" and "circuit" approaches is provided, which has established that "conditional" losses correspond to losses in rails, train carriages, and electric locomotives.

Keywords: power losses; electric traction; train; current; electromagnetic field strength; inter-substation zone; carriage; rails; contact wire; electric locomotive

1. Introduction

Electric traction systems are among the largest consumers of electric power. Therefore, it is essential to use them economically and reduce power losses for the sake of rapidly growing environmental pollution, limited non-renewable energy sources, and the necessity to increase energy efficiency. At the same time, the existing approaches and methods for electricity loss estimation in grids are the weakest link in the overall energy balance calculation circuit. In our opinion, this is due to the fact that traditional methods for analysis and reduction in energy losses in electric traction networks are based on the "circuit" approach, that is, on the theory and electrical appliances of electrical circuits, which follows from the analysis of publications [1–8]. This article continues and expands on the researches outlined in [9,10]. Let us summarise them shortly.

In [9], a "field" approach based on the theory of the electromagnetic field was proposed and theoretically substantiated for the analysis of the electromagnetic energy transfer from a traction substation (TS) to an electric rolling stock (ERS) through the airspace of inter-substation zones of AC electric traction power supply systems (TPSs). The approach is based on the fundamental law of electromagnetic energy propagation, i.e., on the fact that energy is distributed not by wires but by dielectrics (in particular, by the air) and is

transmitted not by current but by electromagnetic waves. It was shown that the electricity required to move trains and trams, propagating through the airspace of the inter-substation zone, enters the electric rolling stock through the roof and bottom of its body, i.e., the electromagnetic energy enters the inside of the electric locomotive through the roof porcelain insulator and through the air holes in the bottom of the locomotive body [9,10]. Based on the "field" approach of electromagnetic energy propagation from the traction substation to the electric rolling stock described in [9], the next research published in [10] showed that the reactive power consumed by the electric rolling stock is characterised by the standing waves formed in the airspace of the inter-substation zone by the superimposition of the waves falling on the elements of electric traction (contact wire, rails, locomotive and car bodies), and the waves reflected from the surfaces of these elements and devices. The authors proposed two ways to reduce the reactive power which arises as a result of the formation of standing waves—either by the "suppression" (damping) of the already formed standing waves or by preventing the formation of reflected waves by the application of special thin film coatings (single or multi-layered) to the surface of these elements of the electric transport system. The last way is the most effective and state of the art method, which is developing in recent publications [11–14].

The article is structured as follows. Section 2 presents a review of the last researches and articles and the current issues connected with the definition of power losses on electrified transport. Section 3 is dedicated to the "field" approach and its theoretical aspects. Section 4 describes the conditions and initial data for active power losses numerical calculations. The results of numerical calculations of power losses in different elements are shown in Section 5 for traction networks, Section 6 for carriages, and Section 7 for the electric locomotive. Finally, Section 8 presents the main conclusions made by authors based on the results of theoretical and numerical analyses.

2. Analysis of Selected Research Studies Dedicated to Power Loss Estimation in Railway Transport

The results of experimental and numerical calculation of electricity losses are shown in [3] on the example of a feeder zone with two TSs equipped with 6-pulse rectifiers. The experimental research was performed with the help of electric meters installed at TSs and ERSs. The load in the experiments was represented by a freight train with a weight of 1879 tons driven by the ET22 electric locomotive. It was found that the average efficiency of the electric power transmission of the feed zone was 87.21%, and total power losses relative to the energy delivered to the TSs were 12.79%.

Paper [4] proposes a method for assessing and minimising power losses in the traction power supply system by voltage regulation of a TS according to the limits described in the EN50163 standard. The problem was solved by computer simulation, which found that to reduce power losses it is advisable to increase the voltage of TS to not more than 1700–1800 V.

Article [5] considers the structure of the imbalance of electric power losses during a train operation, which reaches up to 17%. Experimental research showed that the annual loss of electricity in TPSs is 13.3%, including losses in step-down transformers of 0.7–1.5% of the nominal volume of electricity received from the external power system and losses in traction transformers of 0.81–1.51% of the energy released for train traction.

The magnetic losses in AC locomotives are investigated in [6]. The authors proposed an improved model which allows one to estimate magnetic losses in the magnetic steel and also in any magnetic material, taking into account their properties, shape, etc. The results of the calculation are presented for electrical steel of 1312 type for different magnetisation frequencies (50 and 60 Hz) based on the NB-418-K5 motor. In addition, the authors performed calculations of efficiency according to different existing procedures and methods to demonstrate potential inaccuracies. The proposed method provides precise results.

Interesting results of measurements and calculations are shown in [7]. The article discusses power loss estimation and reduction in TPSs of the East Japan Railway Company,

fed from a 154 kV power line. The following are proposed as measures to reduce power losses in TSs: introduce a high-efficiency rectifier, voltage regulation, use lithium-ion batteries in energy recovery modes, replace air conditioners, and implement LED lighting.

Using the classical modelling method, [8] calculates power losses in TPSs with various supply voltages (V): 1500, 3000, 6000, and 9000. It was found that when the supply voltage is raised from 1500 to 3000 V, power losses decrease by 25%.

The author of [15,16] demonstrates that the existing indirect methods for determining electrical energy losses ΔW in the contact line have an error of about 7.5%. This is due to the fact that the existing methods are based on the expression below

$$\Delta W = k_l \int_0^T I_f^2(t)dt$$

which calculates the losses using the value of feeder current I_f and energy losses coefficient k_l; the latter could be determined only imprecisely. Therefore, the author proposed and improved the indirect method by considering the influence of six significant factors on the value of k_l. Some of them include the power supply circuit of the catenary system, the number of trains in the inter-substation zone, the contact wire wear, and ERS movement speed. Based on a full factorial experiment $2n$, a regression equation was obtained to estimate the loss coefficient k_l from which it follows that the number of trains moving along the inter-substation zone has the most significant influence on k_l. The proposed technique for assessing k_l allowed for increasing the accuracy of power loss estimation by 5.13% [15,16].

As follows from the publications analysed above [1–8] and also many other publications, which are not mentioned in the article, the assessment of power losses in the TPS is carried out either by calculation (analytical or modelling) or experimentally by power meters installed on TSs and ERSs. In the former case, the calculated input data are the electrical parameters and currents in the catenary system, and in the latter case, the currents and voltages of the corresponding electrical circuits of the TS and ERS. Such a solution to the problem is explained by the fact that it is traditionally believed that electricity propagates from the TS to the ERS along the wires of the catenary system and is transferred by the electric current flowing through these wires. However, it is well established that according to the fundamentals of theoretical electrical engineering, the electromagnetic energy is transmitted from a source to a consumer not through the wires of an electrical circuit but through a dielectric, and is transferred not by the movement of charged particles (not by current), but by electromagnetic waves, i.e., an electromagnetic field with the speed of 3×10^8 m/s. In our opinion, the failure to take into account this fundamental law of electricity distribution leads to the fact that until now, electrical specialists cannot establish the "true" electricity costs in electric traction systems. Thus, calculations and readings of power meters for electricity consumption for train traction (i.e., for a TS and an ERS) differ significantly, and the variation sometimes reaches 28%. These "difference leakages" of electricity are even given the name "conditional loss", the hopelessness of which is emphasised by the fact that they are even regulated by directives [17]. Conditional losses reach quite significant percentages and are equal in average up to 15.1% in an AC electric traction system. Although the authors of [17] tried to substantiate the factors of the appearance and the dynamics of changes in these losses, in our opinion, the arguments they use are unconvincing.

In this regard, the authors of this article propose a new so-called "field" approach to assess power losses in electric traction systems; that is, an approach based on the theory of the electromagnetic field, according to which the transmission of electricity by quantity and direction is characterised by the Poynting vector $\vec{S}$ [9,10]:

$$\vec{S} = \left[\vec{E} \times \vec{H}\right],$$

where: $\vec{E}$ and $\vec{H}$ are the electric and magnetic field strength vectors at the points of the dielectric or devices in the inter-substation zone of the AC electric traction system.

Works [18,19] have significant theoretical and practical investigations dedicated to waves propagation in the overhead wires and accurate calculations of magnetic field intensity in general applications. At the same time, a significant number of publications, for example [20–27], present the results of determining, by calculation or experiment, the strengths of electric $\vec{E}$ or magnetic $\vec{H}$ fields at various points in the spaces of electric traction systems. However, the energy properties and functions of these fields are not considered.

In particular, [20,21] present the results of measurements of low-frequency magnetic field strength on two DC transformers. The measurements were performed inside TS buildings, at points around the 6-pulse rectifier, and outside a TS in the area surrounding the 132 kV external power transmission line. The H-field spectra present measurement results in the frequency ranges from 30 to 430 Hz and from 430 Hz to 12 kHz. The amplitudes of the H-field inside the buildings for the 3rd (12 A/m), 6th (13 A/m), and 12th (13 A/m) harmonics were established. Outside the TS buildings, the 6th and 12th harmonics had amplitudes of 13 A/m. The resulting strength of the B-field was around 5 nT, which is below the regulatory limit of human exposure.

Similar estimates [22] of the level of the B-field were also performed by Italian researchers at points 10 m away from a high-speed railway line electrified by 25 kV, 50 Hz. The values of magnetic induction are provided during train movement at a speed of 250 km/h at a current of 390 A. The maximum value of the vector reached 1.9 T, and the most probable value was 0–1 T. The probability of value $B = 3$ T did not exceed 0.03, and the median value was 0.64 T.

To determine the effect of the alternating magnetic field generated by the current in the rails on inductive wheel sensors, the South African Railway Company (Spoornet) funded an experimental study to estimate the level of the B-field around the rail with an alternating current of 600 A, 50 Hz [23]. As a result, it was found that in the region where the sensor is located, the values of induction B are in the range of 16.0 to 11.5 mT, with a maximum possible value of 19.0 mT.

In [24], magnetic induction around the wires of the AC catenary system was determined by analytical calculations known from theoretical electrical engineering, with the use of the mirror image method. It was found that induction B reaches 21.0 mT at a distance of 3.5 m from the wire with a current of 170 A.

The methods for approximate calculations of the strengths of electric and magnetic fields in the airspace of a DC-electrified section were proposed in [25] based on the method of superposition well established in theoretical electrical engineering.

Authors of the publication [26], using the modelling method of a high-frequency electromagnetic field generated near air networks and railway equipment, showed that a train consuming a current of 200 A generates a voltage of 154 V on a 10 km-long line.

Paper [27] shows the results of a study dedicated to the application of magnetic field energy harvesting located closely to the railway track of Norwegian railways with a voltage of 15 kV AC, 16.7 Hz. The possibility of accumulation of sufficient energy in the magnetic field is analysed to extend the lifetime of distributed condition monitoring systems used in such infrastructure as bridges, tunnels, rails, etc. The study showed that a train driven by the Rc8 locomotive receiving a current of $I_{rms} = 100$ A creates a magnetic field with induction at a distance of 0.5 m from the rail and $B = 25$ µT. This field strength is sufficient to accumulate the energy in the storage device, making it possible to increase the service time of the existing monitoring systems significantly.

Many more publications which estimate the level of the electromagnetic field—mainly its magnetic component created by the electric traction network—could be cited and analysed. However, the primary goal of such publications and those analysed above is to assess the magnitude of possible impacts of such a field on people (which is quite understandable and natural) located in its space. Yet, the electromagnetic field (electromagnetic waves) is created and propagated throughout the space of inter-substation zones of the electric trac-

tion system. Therefore, it covers and energetically affects all elements of the TPS, including the main "productive" object of the system—a moving train. This influence is undoubtedly significant from the technical and economic point of view to estimate the energy-efficient operation of electric traction systems.

This article aims to develop and theoretically substantiate a new method for determining active power losses in the devices of electric traction systems based on the existing theory of the propagation of electromagnetic field energy in dielectric and conductive media.

3. Theoretical Aspects of the "Field" Approach

Let us consider the inter-substation zone of the AC electric traction system with several freight trains being in operation. The space of the inter-substation zone is conditionally limited by the traction substation, traditional suspension catenary and rails. Additionally, let us assume that according to the electromagnetic characteristics (σ, ε_a, μ_a) this space is linear, homogeneous, isotropic, and does not contain external electric motive forces (EMF) and free charges.

In the dielectric space (i.e., the inter-substation zone's airspace), the electromagnetic field is created by currents flowing in the traction network and the voltage between the catenary and the rails. At the same time, electromagnetic waves propagating in the airspace of the inter-substation zone meet catenary wires, electric rolling stock, carriages, and rails on their way. They are partially reflected from the surfaces of these structures [9,10], and partly they penetrate and dissipate in them in the form of heat losses, the determination of which is the primary purpose of this article.

To solve the problem based on the "field" approach, we must establish the coordinate system in which to perform the calculations of the strengths of the electric $\overrightarrow{E}$ and magnetic $\overrightarrow{H}$ fields, considering the shape of the contact suspension and the rails.

Let us represent the overhead contact system (catenary) of PBSM2-95+MF-100 type used in the investigated electric traction system by a single equivalent contact wire with a cross-section of 193.3×10^{-6} m^2 [28] and cylindrical shape with a radius of $r_c = 0.00785$ m. Its specific electrical conductivity is $\sigma_c = 3.82 \times 10^7$ S/m and relative magnetic permeability is $\mu_{rc} = 10$. Let us assume that the feeder voltage and current in normal operation modes are sinusoidal, with frequency equal to $f = 50$ Hz. Then the penetration depth δ_c of a harmonic electromagnetic wave with a frequency of 50 Hz into the surface of the equivalent contact wire will be equal to:

$$\delta_c = \sqrt{\frac{2}{\omega \cdot \sigma_c \cdot \mu_{ac}}}, \text{i.e., } \delta_c = 3.64 \text{mm and } \delta_c < r_c.$$

Similarly, let us replace both rails of R65 type by a single equivalent rail with a cross-section of 1.65 m^2 [28–30] and cylindrical shape with radius of $r_r = 0.0727$ m. Its specific electrical conductivity is $\sigma_r = 8 \times 10^6$ S/m, and relative magnetic permeability is $\mu_{rr} = 1000$. Then the depth of penetration of an electromagnetic wave into the surface of the equivalent rail is equal to:

$$\delta_r = \sqrt{\frac{2}{\omega \cdot \sigma_r \cdot \mu_{ar}}}, \text{i.e., } \delta_r = 0.796 \text{ mm and } \delta_r < r_r.$$

From the resulting inequalities ($\delta_c < r_c$ and $\delta_r < r_r$) it follows that the electromagnetic fields of inside layers with thicknesses of δ_c and δ_r would be the same as if the layers had a flat shape. Then, for the equivalent contact wire and rail, all relationships established for the case of a flat dielectric-conductor interface are valid. This makes it possible to solve the set electromagnetic problem in the Cartesian coordinate system.

An alternating electromagnetic field with a frequency of 50 Hz in the conductive media of devices in the inter-substation zone is described by the following system of equations for instantaneous electromagnetic quantities [31,32]:

$$rot\vec{H} = \sigma\vec{E},$$
(1)

$$rot\vec{E} = -\mu_a\frac{\partial\vec{H}}{\partial t},$$
(2)

$$div\vec{E} = \frac{\rho}{\varepsilon_a},$$
(3)

$$div\vec{H} = 0.$$
(4)

Let us perform the *rot* operation from both sides of Equation (1):

$$rot\ rot\vec{H} = \sigma\ rot\ \vec{E}.$$
(5)

Considering the replacement of the operation *rot rot* in Equation (5) and the substitution of Equation (2) into Equation (5), we obtain:

$$grad\ div\vec{H} - \nabla^2\vec{H} = -\sigma\ \mu_a\ \frac{\partial\vec{H}}{\partial t}.$$
(6)

Considering relation in Equation (4), we obtain the simplest homogeneous d'Alembert equation for $\vec{H}$:

$$\nabla^2\vec{H} - \sigma\ \mu_a\ \frac{\partial\vec{H}}{\partial t} = 0.$$
(7)

Let us consider a plane wave for strength $\vec{H}$, propagating along the 0 Z axis, in the Cartesian coordinate system, perpendicular to the conductive surfaces of the studied devices of the inter-substation zone. Then, Equation (7) could be simplified to

$$\frac{\partial^2\vec{H}(z,t)}{\partial z^2} - \sigma\ \mu_a\ \frac{\partial\vec{H}(z,t)}{\partial t} = 0.$$
(8)

Electromagnetic waves in the inter-substation zone are excited by the sinusoidal voltage and current of the traction network, so strengths $\vec{E}$ and $\vec{H}$ will also be harmonic functions. Then, Equation (8) could be written in a complex form as

$$\frac{d^2\underline{H}}{d z^2} - j\omega\sigma\mu_a\ \underline{H} = 0.$$
(9)

As it is known, Equation (9) has a solution:

$$\underline{H}(z) = \underline{A}_1 e^{-\underline{\gamma}\ z} + \underline{A}_2 e^{\underline{\gamma}\ z},$$
(10)

where: $\underline{A}_1$ and $\underline{A}_2$ are constants of integration; γ is a wave propagation coefficient.

The electric field strength is determined based on Equation (1) as

$$\vec{E} = \frac{1}{\sigma}rot\ \vec{H},$$

and for a plane wave as

$$rot\ \underline{H} = -\vec{i}^0\frac{1}{\sigma}\frac{d\underline{H}}{dz}$$

i.e., this means that:

$$\underline{E} = -\vec{i}^0 \frac{1}{\sigma} \frac{d\underline{H}}{dz}. \tag{11}$$

After differentiation of Equation (10) and its substitution into Equation (11), we obtain the following:

$$\underline{E}(z) = \underline{Z}_c \underline{A}_1 e^{-\gamma z} - \underline{Z}_c \underline{A}_2 e^{\gamma z}, \tag{12}$$

where: $\underline{Z}_c$ is the wave complex resistance of the conducting medium of the devices of the inter-substation zone, which could be defined as

$$\underline{Z}_c = \frac{\gamma}{\sigma} = \sqrt{j\frac{\omega\mu_a}{\sigma}} = \sqrt{\frac{\omega\mu_a}{\sigma}} \cdot e^{j45°} = Z_c e^{j45°}, \tag{13}$$

where

$$\underline{\gamma} = \sqrt{j\omega\sigma\mu_a} = \sqrt{\omega\sigma\mu_a} e^{j45°} = \alpha + j\beta.$$

Let us use the boundary conditions described below to determine the constants of integration $\underline{A}_1$ and $\underline{A}_2$ in Equations (10) and (12).

As was found above, the radii of the equivalent contact wire and rail are greater than the wave propagation depth. Similarly, it can also be shown that the thicknesses of the steel sheets of the electric locomotive bodies (5 mm) and train carriages (3 mm) exceed the wave attenuation depth (0.736 mm). Therefore, these devices of the inter-substation zone can be considered infinite electrically conductive half-spaces ("impervious" to electromagnetic waves). Then *the first boundary condition* is that for the value of the coordinate $z \to \infty$, the values of $H(z) = 0$ and $E(z) = 0$. Then Equations (10) and (12) will take the following form:

$$\underline{H}(\infty) = 0 = \underline{A}_1 e^{-\gamma \cdot \infty} + \underline{A}_2 e^{\gamma \cdot \infty}, \tag{14}$$

$$\underline{E}(\infty) = 0 = \underline{Z}_c \underline{A}_1 e^{-\gamma \cdot \infty} - \underline{Z}_c \underline{A}_2 e^{\gamma \cdot \infty}. \tag{15}$$

From the system of Equations (14) and (15) it follows that under the above-mentioned condition, the constant $\underline{A}_2$ must be equal to zero ($\underline{A}_2 = 0$), otherwise, the strengths $H(\infty)$ and $E(\infty)$ will not take zero values, but infinitely large values, which does not happen in practice (i.e., it is impossible).

The second boundary condition for the surfaces of the devices under study, we could find for $z \to 0$. Then, Equations (10) and (12) will be written for $\underline{A}_2 = 0$ in the following form:

$$\underline{H}(0) = H_S = \underline{A}_1 e^{-\gamma \cdot 0} = \underline{A}_1, \tag{16}$$

$$\underline{E}(0) = E_S = \underline{Z}_c \underline{A}_1 e^{-\gamma \cdot 0} = \underline{Z}_c \underline{A}_1, \tag{17}$$

where H_S and E_S are the strengths of the magnetic and electric fields on the surface of the contact wire, rail, carriage bodies, locomotive, etc.

Considering the obtained values $\underline{A}_1$ and $\underline{A}_2$, the resulting system of equations of the electromagnetic field in the conductive media of the devices of the inter-substation zone will be written in the following form:

$$\underline{H}(z) = H_S e^{-\gamma z}, \tag{18}$$

$$\underline{E}(z) = \underline{Z}_c H_S e^{-\gamma z}. \tag{19}$$

Having available the dependencies $\underline{H}(z)$, $\underline{E}(z)$, and Equation (13) for $\underline{Z}_c$, we could write the expression for the Poynting vector in complex form as

$$\underline{S} = [\underline{E}(z)\underline{H}''(z)] = \underline{Z}_c H_S e^{-\gamma z} H_S e^{\gamma z} == \underline{Z}_c H_S^2 = \sqrt{\frac{\omega\mu_a}{\sigma}} e^{j45°} H_S^2 = \sqrt{\frac{\omega\mu_a}{2\sigma}} H_S^2 + j\sqrt{\frac{\omega\mu_a}{2\sigma}} H_S^2, \tag{20}$$

where H_S is the effective value of the magnetic field strength on the surface of the device under study.

Finally, the expression for power losses per unit surface of the device will be determined as the real part of Equation (20) for $\underline{S}$ and will be [W/m^2]:

(a) for non-magnetic materials:

$$P = \sqrt{\frac{\omega \mu_a}{2\sigma}} H_S^2, \tag{21}$$

(b) for magnetic materials (considering non-linearity $\mu_a(H)$ and hysteresis losses):

$$P = 1.4 \sqrt{\frac{\omega \mu_a}{2\sigma}} H_S^2. \tag{22}$$

4. Conditions for Numerical Calculations of Power Losses

Let us perform numerical calculations of active power losses in the devices and elements of the inter-substation zone mentioned above with unilateral supply (in this case, the power losses will be maximum, and we will determine them), i.e., in equivalent contact wire, locomotives, carriages, and equivalent rail.

Four freight trains operate in this zone, with 57 universal covered 4-axle carriages of the 11-270 model. Each train is driven by AC 50 Hz electric locomotives of DS3 type (manufactured by Dniprovskiy Electric Locomotive Building Plant in Ukraine), taking a load current $I_p = 208.9$ A, power $P_p = 5369$ kW, and having the pantograph voltage $U_p = 26,120$ V. Let us assume that the trains are of the same type, located at the same distance of 12 km from each other. At some point, their location corresponds to the schematic shown in Figure 1.
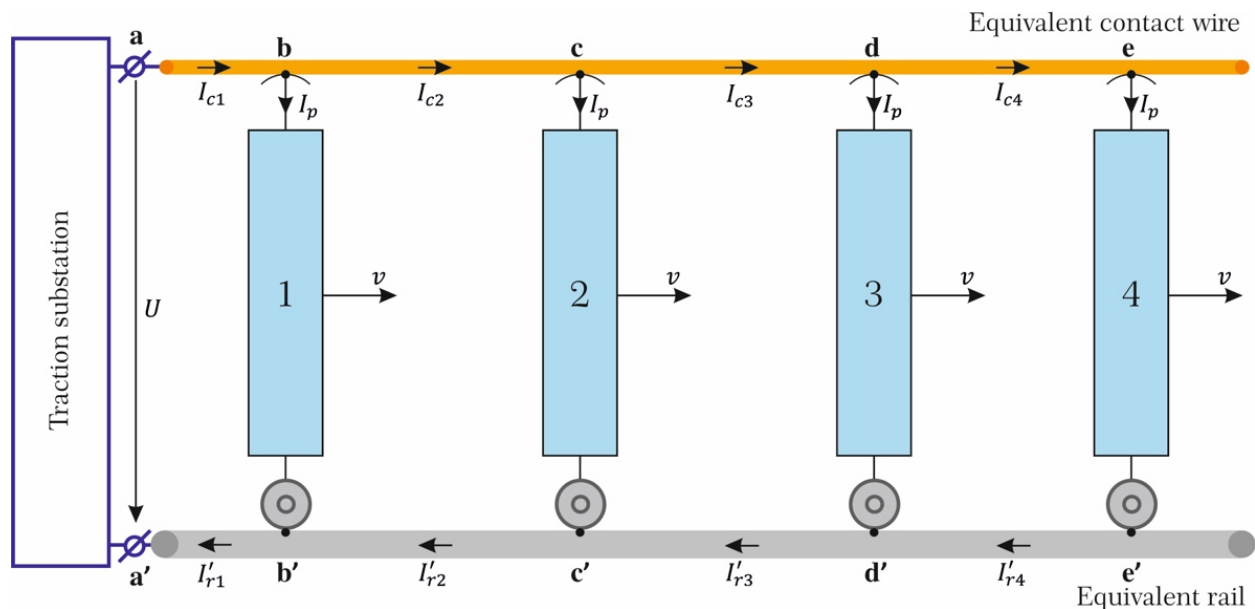

Figure 1. Schematic representation of the AC inter-substation zone with one-sided power supply and four trains driven by DS3 locomotives.

In this case, according to Kirchhoff's first law, the currents in sections **ab, bc, cd,** and **de** of the catenary (i.e., equivalent contact wire) will be equal to $I_{c1} = 835.6$ A, $I_{c2} = 626.7$ A, $I_{c3} = 417.8$ A, and $I_{c4} = 208.9$ A. At the same time, according to different publications [33–36], the proportion of currents flowing in the track circuits of the AC electric traction system could vary in a very wide range up to 50–60% of the current in the catenary. The nature of stray (earth) return current transmission in itself is a complicated enough topic because of different factors. There are many approaches for the calculation

of stray currents in railway traction, depending on the type of section, load, and other factors. There may also be different underground infrastructure: a continuous pipeline (without interruptions), and a separate pipeline, with and without active protection against corrosion. The stray currents also vary with soil resistivity. In addition to the fact that the earth is a good suppressor of electromagnetic waves [37], the leakage currents flowing in the ground will not be clustered, as in rails, but will spread over the metal infrastructure, forming a more scattered and rather weak magnetic field than in rails where the field will be clustered (concentrated) on a small plane. All of this causes a multitude of options both for calculating the stray current itself and for the losses associated with the transfer of energy by an electric field. The solution to this problem requires an integrated approach and can be the subject of future articles. In view of this, the leakage current is not considered in this article as an issue that requires separate and in-depth research [10]. Assuming that the return current proportion is around 55%, the currents in the corresponding sections **a′b′**, **b′c′**, **c′d′**, and **d′e′** of the rails (i.e., equivalent rail) are $I'_{r1} = 459.58$ A, $I'_{r2} = 344.69$ A, $I'_{r3} = 229.8$ A, and $I'_{r4} = 114.9$ A.

Power losses in the equivalent contact wire were determined by Equation (21), and in the equivalent rail, steel roof sheets of the electric locomotive and carriages, as well as in the steel sheets of the carriage bottoms according to Equation (22). At the same time, the necessary values of the magnetic field strength H_S on the surfaces of these devices and elements were estimated by various methods depending on their shapes and physical dimensions. The assumed parameters of the studied devices of the inter-substation zone are provided in Table 1.

Table 1. Parameters of devices and elements of the inter-substation zone.

Device or Element of Inter-Substation Zone	Parameters of Metal Device or Element		
	Electrical Conductivity $\sigma \times 10^6$ [S/m]	Relative Magnetic Permeability μ [r.u.]	Radius or Thickness [mm]
Equivalent contact wire	38.2	10	7.85
Equivalent rail	8	1000	72.7
Electric locomotive, steel sheet	0.2–1.8	5200	5
Carriages, sheet steel	0.2–1.8	5200	3

5. Power Losses in Traction Network

The assessment of power losses in the contact suspension of the inter-substation zone was performed according to Equation (21) for each section **ab**, **bc**, **cd,** and **de** in Figure 1 of the equivalent contact wire with the parameters given in Table 1. The required values of the magnetic field strength H_{Scn} on the surface of the n-th section with current I_{cn} were determined according to the law of total current:

$$H_{Scn} = \frac{I_{cn}}{2\pi r_{cn}}, \tag{23}$$

where $r_{cn} = 0.00785$ m is the radius of the equivalent contact wire, the surface of which in each n-th section S_{cn} with the length of $l_{cn} = 12 \times 10^3$ m could be defined as:

$$S_{cn} = 2\pi r_{cn} l_{cn}, \text{ i.e., } S_{cn} = 591.58 \text{ m}^2.$$

Similarly, but using Equation (22), we evaluated power losses in the rails: by determining them for the equivalent rail in each section **a'b'**, **b'c'**, **c'd',** and **d'e'** in Figure 1 with the corresponding current. The "active" surface (75%) of each section of the equivalent rail equals 4109.0 m^2.

The results of power loss calculation in the equivalent contact wire and rail are shown in Tables 2 and 3.

Table 2. Power losses in the equivalent contact wire.

Sections of the Equivalent Contact Wire		ab	bc	cd	de
Currents in the sections [A]		835.6	626.7	417.8	208.9
Magnetic field strength H_S [A/m]		16950	12713	8475	4238
Power losses	specific [kW/m^2]	1.846	1.038	0.462	0.116
	total [kW]	1092.1	614.2	273.3	68.62

Table 3. Power losses in the equivalent rail.

Sections of the Equivalent Rail		a'b'	b'c'	c'd'	d'e'
Currents in the sections [A]		459.58	344.69	229.8	114.9
Magnetic field strength H_S [A/m]		1006.6	755	503.3	251.7
Power losses	specific [kW/m^2]	0.223	0.126	0.056	0.014
	total [kW]	916.31	517.7	230.1	57.53

6. Power Losses in Steel Sheets of Carriage Roofs and Bottoms

The sheathing of the upper parts (roofs) and lower parts (bottoms) of carriage body frames of 11-270 type is made of the 10X NDP low-alloy steel grade 3 mm thick and with magnetic permeability $\mu_r = 5200$. The penetration depth of an electromagnetic wave with a frequency of 50 Hz into such sheets is 0.736 mm. Thus, the sheets of roofs and bottoms of carriages can be considered infinite electrically conductive half-spaces. In this regard, magnetic field strengths on the surface of roofs and bottoms, necessary for estimating power losses in them according to Equation (22), were determined by the mirror image method well established in theoretical electrical engineering [32,38]. In this case, the equivalent contact wire and, accordingly, the equivalent rail could be represented as in Figure 2.
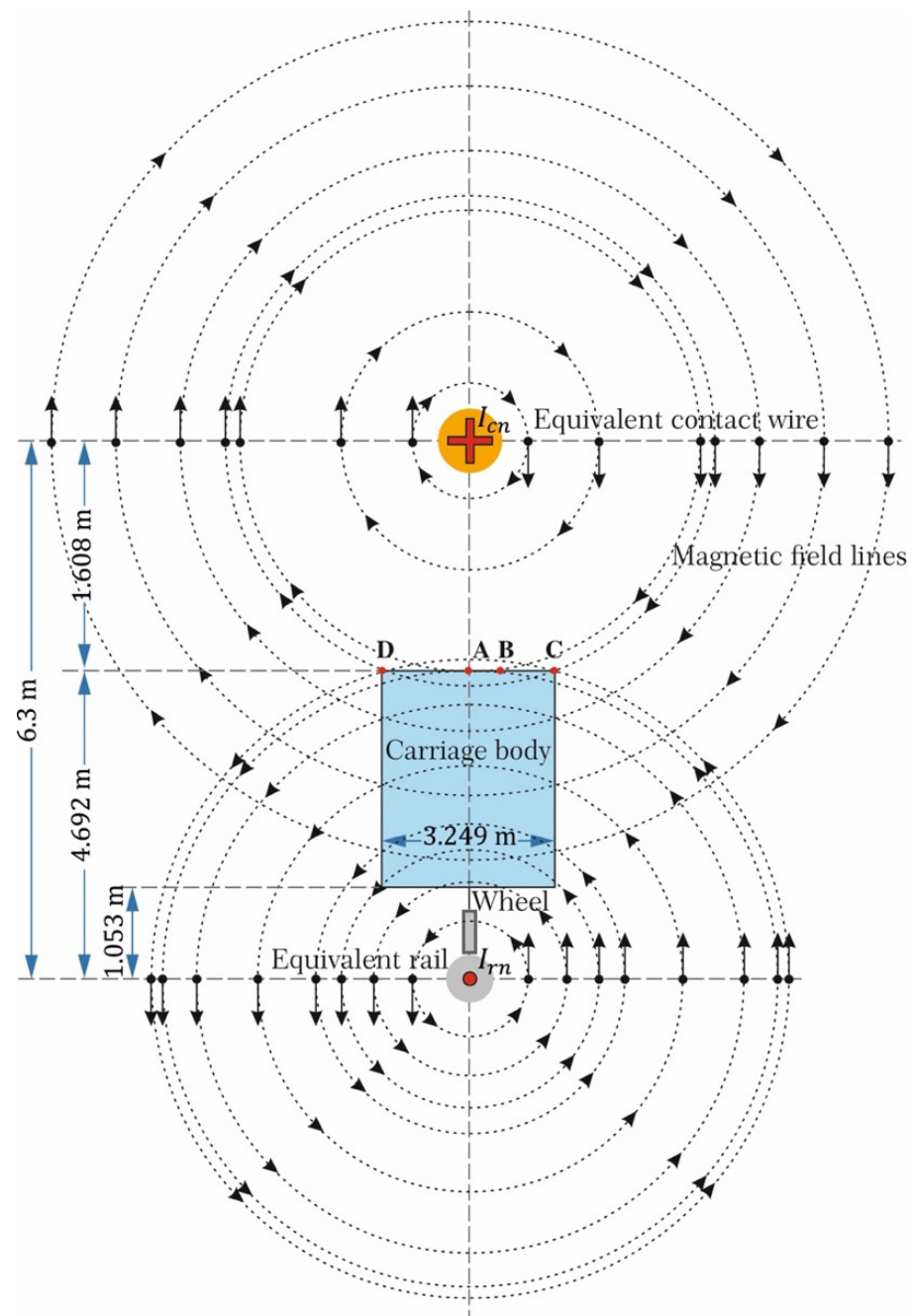
Figure 2. Schematic representation of magnetic field lines created by traction current flowing in the equivalent contact wire and rail propagating in the space of the AC inter-substation zone and penetrating the carriage body.

To solve the task of power losses estimation in the steel sheets of the carriage roof, it is necessary to determine H_S on the surface **CD** shown in Figures 2 and 3. This strength is equal to the difference between the tangential components of the corresponding total strengths $\vec{H}_{1\tau}$ and $\vec{H}_{2\tau}$ according to Figure 3 with the mirror image I_{2cn} of the current in the contact wire I_{1cn}:
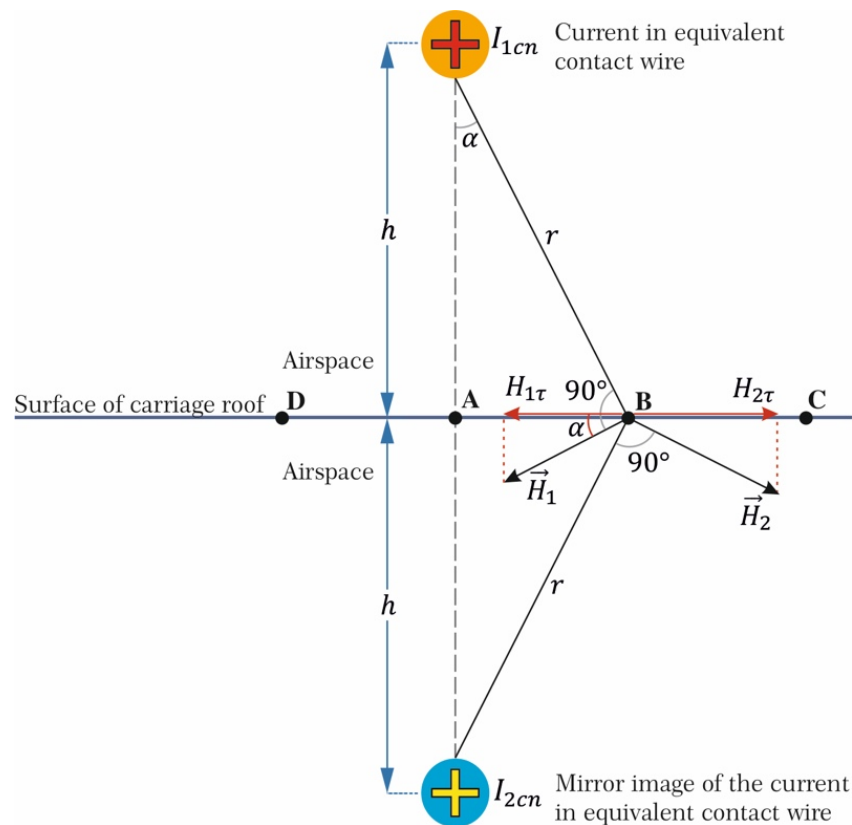
$$H_S = H_{1\tau} - H_{2\tau}. \tag{24}$$

Figure 3. Calculation scheme for the mirror image method of the magnetic field on the roof surface of the carriage, created by the traction current in the equivalent contact wire.

Therefore, the strengths $\vec{H}_1$ and $\vec{H}_2$, created by currents I_{1cn} and I_{2cn}, are separated by the expression of the total current law (analogically to Equation (23)), respectively, as:

$$H_1 = \frac{I_{1cn}}{2\pi r},\tag{25}$$

$$H_2 = \frac{I_{2cn}}{2\pi r}.\tag{26}$$

The dependences $H_1(r)$ and $H_2(r)$ are equilateral hyperbolas, which determine the uneven hyperbolic distribution of the H_1 and H_2 values, and also $H_{1\tau}$, $H_{2\tau}$, and H_S on the surface of the carriage roof. Hence, when assessing H_S as the calculation point **B** (Figures 2 and 3) on the roof **CD**, the abscissa **AB** (we denote it as l) has to be taken equal to the median value of the distribution of the strengths. Calculations give the following result

$$\mathbf{AB} = l = 0.1\mathbf{AC} = 0.162 \text{ m.}$$

Subsequently, calculations were carried out according to Figure 3 as follows. Let us define current image I_{2cn}:

$$I_{2cn} = M_q I_{1cn},\tag{27}$$

where: M_q is the mirror image coefficient of alternating current [38] equal to

$$M_q = \frac{\mu_{qr2} - \mu_{r1}}{\mu_{qr2} + \mu_{r1}},\tag{28}$$

where: μ_{r1} is the relative magnetic permeability of the air space above the carriages, and it equals 1; μ_{qr2} is the fictitious relative magnetic permeability of a massive ferromagnet, and it equals 1.5 [38] in our task for the steel sheet of the carriage roof.

Therefore, according to Equations (27) and (28): $I_{2cn} = 0.2I_{1cn}$ and $M_q = 0.2$. From the right triangle in Figure 3 for $h = 1.608$ m and $\mathbf{AB} = l = 0.162$ m, we find that $r = 1.65$ m and $\mathrm{tg}\alpha = 0.1$; then $\alpha = 5.7°$ and $\cos\alpha = 1$.

Further, the application of Equations (25) and (26) and the obtained figures allow us to determine the tangential components of the strengths $H_{1\tau}$ and $H_{2\tau}$:

$$H_{1\tau} = \frac{I_{1cn}}{2\pi r}\cos\alpha = 0.1I_{1cn},$$

$$H_{2\tau} = \frac{I_{2cn}}{2\pi r}\cos\alpha = 0.02I_{1cn}.$$

As a result, the expression of the desired resulting magnetic field strength on the carriage roof surface will take the form:

$$H_s = H_{1\tau} - H_{2\tau} = 0.08I_{1cn}. \tag{29}$$

Further, substitute into Equation (29) the values of the currents in the contact wire I_{c1}, I_{c2}, I_{c3}, and I_{c4} shown in Figure 1. We obtain the values of H_s on the surface of the roof of the carriages of the corresponding train. The specific and the total power losses on the surfaces (area 2568.63 m^2) of roofs of 57 carriages of the corresponding train are possible to determine by Equation (22). The results of the calculation are presented in Table 4.

Table 4. Calculation of power losses in the steel sheets of carriage roofs and bottoms.

Train Number with Carriages According to Figure 1		1	2	3	4
Magnetic field strength on the surface [A/m] of	roofs	66.85	50.14	33.42	16.7
	bottoms	55.15	41.36	27.6	13.8
Specific power losses [W/m^2] in	roofs	149.3	84.0	37.3	9.33
	bottoms	101.6	57.14	25.14	6.35
Total power losses [kW] in	roofs	383.4	215.65	95.85	24.0
	bottoms	260.9	146.8	65.3	16.3

In addition, calculations of power losses in the steel sheets of the carriage bottoms were performed by the mirror image method according to a similar technique and using the geometric dimensions of Figure 2; the results are shown in Table 4.

7. Power Losses in Steel Sheets of Roofs of Electric Locomotives

The roofs of electric locomotives are made of steel sheets 5 mm thick; the depth of electromagnetic waves with a frequency of 50 Hz is 0.736 mm. That is, the roofs of electric locomotives are infinite electrically conductive half-spaces.

The electromagnetic wave, created by the current in the contact wire I_c and the current flowing in the current collector (pantograph) I_p (Figure 4), fall on the roof surface with dimensions of 17×3.1 m for each electric locomotive. This requires determining the magnetic field strength $\vec{H}_S$ on the surface of the roofs of electric locomotives by superimposing two components: $\vec{H}_S = \vec{H}_{Sc} + \vec{H}_{Sp}$. The component $\vec{H}_{Sc}$ of the current in the contact wire was determined (similarly to the roofs of the carriages) by the mirror image method according to the geometric dimensions of Figure 4a, and specific power losses, according to Equation (22). Total losses for a single electric locomotive were found for the surface area of the roof of the electric locomotive being 52.7 m^2; calculation results are given in Table 5.
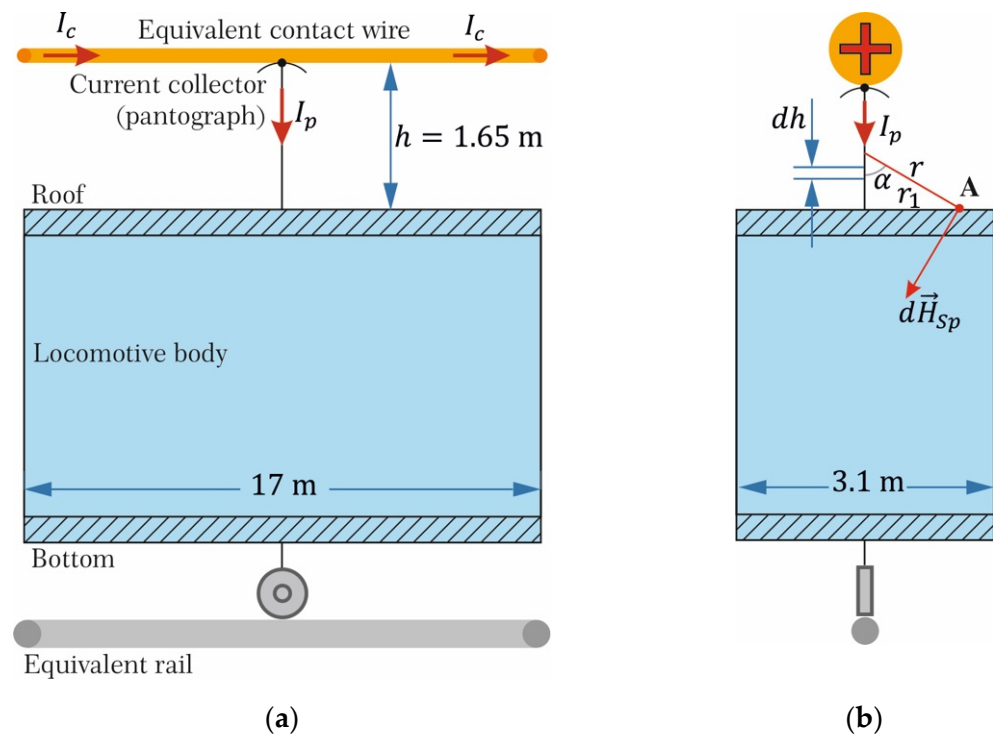
Figure 4. Calculation schematic for the superimposition and mirror image methods of the magnetic field on the roof of the electric locomotive created by currents in the equivalent contact wire and the current collector (pantograph): (**a**) side cross-section; (**b**) front cross-section.

Table 5. Calculation of power losses in the steel sheets of the locomotives' roofs and bottoms.

Train Number with Carriages According to Figure 1		1	2	3	4
Current I_c in Figure 4a [A]		835.6	626.7	417.8	208.9
Magnetic field strength H_{Sc} [A/m]		64.5	48.38	32.26	16.13
Power losses	specific [kW/m^2]	139.0	78.18	35.8	8.95
	total [kW]	7.33	4.12	1.9	0.471

Let us estimate component $\vec{H}_{Sp}$ from the current in the current collector using the Biot–Savart differential law, according to which the current I_p in the element dh of the current collector (Figure 4b) creates tension at point **A** of the roof surface according to the equation below [38]:

$$d\vec{H}_{Sp} = \frac{I_p}{4\pi r^3}\left[d\vec{h}\,\vec{r}\right]; dH_{Sp} = \frac{I_p \sin\left(d\vec{h}\,\vec{r}\right)}{4\pi r^2}dh = \frac{I_p \sin\alpha}{4\pi r^2}dh. \tag{30}$$

Then, magnetic field strength H_{Sp} at any point of the roof surface from the current I_p in the current collector with height h (Figure 4b) could be determined as:

$$dH_{Sp} = \frac{I_p}{4\pi r^2}\int_0^h \sin\alpha\, dh = \frac{I_p}{4\pi r_1}.$$

As a result of the foregoing, we obtain that the electromagnetic wave with strength $H_{Sp\ in}$ falls on the surface of the roofs. This wave is reflected from the surface of the roofs, superimposed on the incident wave, and determines the resulting tension

$$H_S = 2H_{Sp\ in} = \frac{I_p}{2\pi r_1},$$

which numerically varies according to the hyperbolic law depending on distance r_1 (Figure 4b). For $I_p = 208.9$ A and roof surface area of one electric locomotive 52.7 m^2 in the range of change r_1 equals 0.005–1.55 m (the end of the roof in one direction), the calculations yielded 48.7 kW of power losses.

8. Discussion of Calculation Results

As it follows from Tables 2–5, power losses in the traction network are 3769.84 kW, including 2048.2 kW in the catenary system and 1721.64 kW in the rails. The power losses in the roofs and bottoms of all carriages of all four trains could reach 1208.2 kW and in the electric locomotive 208.62 kW. For active power spent on train traction equal to 21,476 kW, the total percentage of power losses in the devices of the inter-substation zone with four moving trains is 24.1% (Table 6). Furthermore, 9.5% are the losses in the catenary system, 8% in the rails, and 6.6% in the roofs and bottoms of carriages and the roofs of electric locomotives. At the same time, it should be noted that power losses in carriages and electric locomotives can be larger due to the components of losses in their side and end surfaces, which are not evaluated in this article.

Table 6. Comparison of calculation results obtained by different approaches.

Total Estimated Power Losses		Power Loss Types			
Calculation Methodology	Percentage [%]	In Catenary System [%]	In Rails [%]	In Carriages and Electric Locomotives [%]	"Conditional" [%]
"field"approach	24.1	9.5	8.0	6.6	–
"circuit"approach	8.83–9.68	8.83–9.68	–	–	15.1

Additionally, we must pay attention to the difference in the total calculated power losses, estimated according to the "field" (24.1%) and "circuit" (8.83–9.68%) approaches. This difference could be explained by the fact that the losses in the "circuit" approach contain only losses in the catenary system since the losses in the rails, as a rule, are usually not determined or are determined inaccurately. This method cannot estimate the losses in the steel sheets of the roofs and bottoms of carriages and electric locomotives. The "conditional" losses are usually applied to compensate for the above difference, but their essence and estimation methods have not been clarified yet. Only in [15,16] is it assumed that one of the reasons, along with others, for the appearance of "conditional" losses is probably the influence of the electromagnetic field on the devices of electric traction systems. In our opinion, and what follows from the figures in Table 6, the "conditional" losses correspond to losses in rails, train carriages, and electric rolling stock. Undoubtedly, such an assumption is fully justified by the loss percentage balance. The so-called "conditional" power losses are losses due to inaccurate and incomplete estimates of total losses performed based on the "circuit" approach.

In conclusion, it should be emphasised that the results of power loss calculations according to the "field" method depend on: the type, shape, and number of carriages in the train; the number of trains in the inter-substation zone; the type and condition of the soil, etc.

9. Conclusions

1. The existing methods and techniques for determining active power losses in railway traction power supply systems are based on the theory of electric circuits (i.e., on the "circuit" approach) and do not take into account the fundamental physical law of propagation and consumption of electromagnetic energy (i.e., the "field" approach). This can lead to erroneous results in the estimation of power losses in the devices of electric traction systems.

2. Electromagnetic waves carrying electric energy from the traction substation to the electric rolling stock, propagating in the airspace of the substation zone, meet on their way electrically conductive devices (catenary system, bodies of locomotives and carriages, rails). The waves partially penetrate them, i.e., are dissipated as heat losses which must be taken into account.

3. In determining power losses in electric traction systems, they need to be examined not only in the electric traction network (in the catenary system and rails) but also in the electrically conductive surfaces of carriages and electric locomotives which meet the wave propagating in the space of inter-substation zone in the process of energy transmission from traction substation to the electric rolling stock.

4. The regularities of propagation of the alternating electromagnetic field in the conductive medium were the basis for obtaining the analytical ratios of active power losses. The losses in the electrically conductive devices of the inter-substation zone of the AC traction power supply system are proportional to the square of the magnetic field strength on the surfaces of these devices. They depend on the type and parameters of these devices.

5. As a result of numerical calculations of power losses in the conducting elements of the feeder zone with four freight trains with 57 carriages in each, it was established that the maximum losses in the one-sided power supply system could reach up to 24.1% of traction power. Furthermore, 14.6% are losses in rails and surfaces of roofs and bottoms of carriages and electric rolling stock, the definition of which became possible only by using the "field" approach method developed by us.

6. What is called "conditional" power losses are total losses in rails, roof surfaces, and bottoms of carriages and electric locomotives, the nature and estimation methods of which have not yet been established, and these are regulated by directives.

7. Theoretical aspects of the analysis and the methodology for determining active power losses in the devices of electric traction systems based on the above "field" approach are applicable not only to all electric transportation systems but also to general industrial electric power systems.

8. The proposed method allows for the estimation of losses created by the magnetic field of feeding and return currents in catenary and rail systems, respectively. The definition of losses created by the return current flowing in the ground infrastructure is not addressed here and has remained a current and complex topic that needs significant further research.

Institutional Review Board Statement: Not applicable.

Informed Consent Statement: Not applicable.

Data Availability Statement: Not applicable.

Conflicts of Interest: The authors declare no conflict of interest.

References

1. Steczek, M.; Jefimowski, W.; Maciołek, T.; Barański, S. Analysis of Energy Losses in the Novel Distributed Power Supply System for Trams. *IEEE Trans. Transp. Electrif.* 2022; Early Access. [CrossRef]
2. Szelag, A.; Kostin, M.; Nikitenko, A. Losses of Recovered Electric Energy in the Elements of a DC Electric Transport System. In Proceedings of the 2016 IEEE International Power Electronics and Motion Control Conference (PEMC), Varna, Bulgaria, 25–28 September 2016. [CrossRef]
3. Chrabąszcz, I.; Kierzyk, M.; Prusak, J.; Boczoń, K. Evaluation of Energy Losses in DC Railway Traction Power Supply System. *Technol. Trans.* **2016**, *2-E/2016*, 109–119. [CrossRef]
4. González, D.; Manzanedo, F. Power Losses Minimization in D.C. Electric Railways by Means of Traction Substations Coordinated Voltage Control. In Proceedings of the IET Conference on Railway Traction Systems (RTS 2010), Birmingham, UK, 13–15 April 2010. [CrossRef]
5. Cheremisin, V.; Nikiforov, M.; Ushakov, S. Assessment of Train Traction Electric Energy Losses. In Proceedings of the 2018 International Multi-Conference on Industrial Engineering and Modern Technologies (FarEastCon), Vladivostok, Russia, 3–4 October 2018. [CrossRef]
6. Goolak, S.; Sapronova, S.; Tkachenko, V.; Riabov, I.; Batrak, Y. Improvement of the model of power losses in the pulsed current traction motor in an electric locomotive. *East-Eur. J. Enterp. Technol.* **2020**, *6*, 38–46. [CrossRef]
7. Hirano, T.; Kikuchi, S.; Suzuki, T.; Hayashiya, H. Evaluation of Energy Loss in D.C. Traction Power Supply System. In In Proceedings of the 2015 17th European Conference on Power Electronics and Applications (EPE'15 ECCE-Europe), Geneva, Switzerland, 8–10 September 2015. [CrossRef]
8. Shigeeda, H.; Morimoto, H.; Ito, K.; Fujii, T.; Morishima, N. Feeding-loss Reduction by Higher-voltage DC Railway Feeding System with DC-to-DC Converter. In Proceedings of the 2018 International Power Electronics Conference (IPEC-Niigata 2018 -ECCE Asia), Niigata, Japan, 20–24 May 2018. [CrossRef]
9. Kostin, M. Electrodynamics of Electric Power Transmission and Losses in Devices of Electric Transport Systems. In Proceedings of the MATEC Web of Conferences, 13th International Conference Modern Electrified Transport—MET'2017, Warsaw, Poland, 5–7 October 2017. [CrossRef]
10. Kostin, M.; Nikitenko, A.; Mishchenko, T.; Shumikhina, L. Electrodynamics of Reactive Power in the Space of Inter-Substation Zones of AC Electrified Railway Line. *Energies* **2021**, *14*, 3510. [CrossRef]
11. Zhao, T.; Teng, W.; Hao, H.; Sun, P.; Liu, Y. Simulation Research on Electromagnetic Shielding Characteristics of Carbon Fiber Car Body for Railway Vehicles. *Procedia Comput. Sci.* **2019**, *154*, 537–542. [CrossRef]
12. Wu, S.; Hou, H.; Xue, X. Photothermal-Thermoelectric Composite Film with Excellent Self-Healing and Low Temperature Resistance Properties for Electromagnetic Wave Shielding and Absorption. *Carbon* **2022**, *196*, 163–175. [CrossRef]
13. Iqbal, A.; Sambyal, P.; Kwon, J.; Han, M.; Hong, J.; Joon Kim, S.; Kim, M.; Gogotsi, Y.; Min Koo, C. Enhanced Absorption of Electromagnetic Waves in $Ti_3C_2T_x$ Mxene Films with Segregated Polymer Inclusions. *Compos. Sci. Technol.* **2021**, *213*, 108878. [CrossRef]
14. Fang, Y.; Wang, W.; Wang, S.; Hou, X.; Xue, W.; Zhao, R. A Quantitative Permittivity Model for Designing Electromagnetic Wave Absorption Materials with Conduction Loss: A Case Study with Microwave-Reduced Graphene Oxide. *Chem. Eng. J.* **2022**, *439*, 135672. [CrossRef]
15. Kyryliuk, T. Improving the Control Method of Energy Losses in Contact Line of Railways. Ph.D. Thesis, Dnipropetrovsk National University of Railway Transport named after Academician V. Lazaryan, Dnipropetrovsk, Ukraine, 2013. (In Ukrainian).
16. Kyryliuk, T. Improving the Control Method of Energy Losses in Contact Line. *Probl. Kolejnictwa* **2015**, *166*, 49–62.
17. Kuznetsov, V.; Serhatyi, Y.; Kyryliuk, T. Experimental Study of "Conditional Losses" in Railway Traction Lines. *East-Eur. J. Enterp. Technol.* **2011**, *4/8*, 29–33. (In Ukrainian) [CrossRef]
18. Carson, J. Wave Propagation in Overhead Wires with Ground Return. *Bell Syst. Technol. J.* **1926**, *5*, 539–554. [CrossRef]
19. Brandão Faria, J.; Almeida, M. Accurate Calculation of Magnetic Field Intensity due to Overhead Power Lines with or without Mitigation Loops with or without Capacitor Compensation. *IEEE Trans. Power Deliv.* **2007**, *22*, 951–959. [CrossRef]
20. Amendolara, A.; Laurenti, G.; Mariscotti, A.; Pozzobon, P. Assessment of H-field Levels Inside a DC Railway Substation. In Proceedings of the IEEE International Symposium on Electromagnetic Compatibility, Washington, DC, USA, 21–25 August 2000. [CrossRef]
21. Mariscotti, A.; Pozzobon, P. Low-Frequency Magnetic Field in DC Railway Substations. *IEEE Trans. Veh. Technol.* **2004**, *1*, 192–198. [CrossRef]
22. Lucca, G.; Moro, M.; Pagani, A.; Zucchelli, L. Measurements of Magnetic Field Produced by the 25kV-50Hz Italian High Speed Railway Line. In Proceedings of the International Symposium on Power Electronics, Electrical Drives, Automation and Motion SPEEDAM 2006, Taormina, Italy, 23–26 May 2006. [CrossRef]

23. Moresco, M.; Cronje, W.; Steyn, B. Modelling and Measurement of Magnetic Fields Around a Railway Track. In Proceedings of the 2004 IEEE Africon. 7th Africon Conference in Africa (IEEE Cat. No.04CH37590), Gaborone, Botswana, 15–17 September 2004. [CrossRef]

24. Liping, Z.; Zhaode, D.; Zhongxi, L. Study on Magnetic Field Distribution for the Catenary System. In Proceedings of the 2010 International Forum on Information Technology and Applications, Kunming, China, 16–18 July 2010. [CrossRef]

25. Apollonskii, S. Estimation of the Electromagnetic Environment on Objects of the Railway Electrified on Direct Current. In Proceedings of the IEEE EUROCON 2009, St. Petersburg, Russia, 18–23 May 2009. [CrossRef]

26. Oancea, C.; Calin, F.; Golea, V. On the Electromagnetic Field in the Surrounding Area of Railway Equipment and Installations. In Proceedings of the 2019 International Conference on Electromechanical and Energy Systems (SIELMEN), Craiova, Romania, 9–11 October 2019. [CrossRef]

27. Espe, A.; Mathisen, G. Towards Magnetic Field Energy Harvesting near Electrified Railway Tracks. In Proceedings of the 2020 9th Mediterranean Conference on Embedded Computing (MECO), Budva, Montenegro, 8–11 June 2020. [CrossRef]

28. Markvardt, K. *Power Supply of Electrified Railways*; Transport: Moscow, Russia, 1982. (In Russian)

29. Keenor, G. Overhead Line Electrification for Railways, 6th ed.; 2021. Available online: https://ocs4rail.com (accessed on 16 June 2022).

30. Szeląg, A. *Electric Traction—Basis*; Oficyna Wydawnicza Politechniki Warszawskiej: Warsaw, Poland, 2020.

31. Cook, D. *The Theory of the Electromagnetic Field*; Dover Books on Physics: New York, NY, USA, 2011.

32. Kostin, M.; Sheikina, O. *Theoretical Foundations of Electrical Engineering*; Dnipropetrovsk National University of Railway Transport named after Academician V. Lazaryan: Dnipropetrovsk, Ukraine, 2001; Volume 3. (In Ukrainian)

33. Milesevic, B.; Filipovic-Grcic, B.; Uglesic, I.; Jurisic, B. Estimation of Current distribution in the Electric Railway System in the EMTP-RV. *Electr. Power Syst. Res.* **2018**, *162*, 83–88. [CrossRef]

34. Szeląg, A. Rail track as a lossy transmission line. Part I: Parameters and new measurement methods. *Arch. Electr. Eng.* **2000**, *49*, 407–423.

35. Szeląg, A. Rail track as a lossy transmission line. Part II: New method of measurements—Simulation and in situ measurements. *Arch. Electr. Eng.* **2000**, *49*, 425–453.

36. Zalesova, O. Theoretical and Experimental Studies of the Electromagnetic Compatibility of AC Roads and High-Voltage Networks of Power Systems in Conditions of Soils with Low Conductivity. Ph.D. Thesis, Peter the Great St. Petersburg Polytechnic University, Saint Petersburg, Russia, 2018. (In Russian).

37. Krakowski, M. *Earth Return Circuits*; Wydawnictwo Naukowo-Techniczne: Warsaw, Poland, 1979. (In Polish)

38. Turovsky, Y. *Technical Electrodynamics*; Energy: Moscow, Russia, 1974.